NOVEL COMPOUND SEMICONDUCTOR DEVICES BASED ON III-V NITRIDES

S. J. PEARTON and C. R. ABERNATHY
University of Florida, Gainesville. FL 32611 USA

F. REN
AT&T Bell Laboratories, Murray Hill. NJ 07974 USA

R. J. SHUL, S. P. KILCOYNE, M. HAGGEROTT-CRAWFORD and J. C. ZOLPER
Sandia National Laboratories, Albuquerque, NM 87185 USA

R. G. WILSON and R. SCHWARTZ
Hughes Research Laboratories

J. M. ZAVADA
U.S. Army Research Office. Research Triangle Park, NC 27709 USA

ABSTRACT

New developments in dry and wet etching, ohmic contacts and epitaxial growth of III-V nitrides are reported. These make possible devices such as microdisk laser structures and GaAs/AlGaAs heterojunction bipolar transistors with improved InN ohmic contacts.

INTRODUCTION

The GaN-AlN-InN materials system offers opportunities to produce electronic and photonic devices with characteristics unobtainable with conventional III-V compound semiconductors[1]. The InGaAlN system allows continuous grading of the bandgap from 1.9 eV to 6.2 eV (InN to AlN) so that green, blue and UV light -emitting diodes and lasers are possible, as well as electronic devices capable of high temperature operation . To date, both blue and green light-emitting diodes are commercially available [2],UV detectors have been reported[3] and a variety of high electron mobility and field effect transistors have been fabricated[4-6]. The performance of these devices is currently limited by the relatively low p-type doping levels achievable in GaN, InGaN and AlGaN and the high contact resistances associated with wide bandgap contact layers. There are also limitations related to the excellent chemical stability of the nitrides which make them difficult to etch ,and the lack of an ion implantation technology ,which would lead to high throughput ,inexpensive FET fabrication schemes.

In this paper we review some of our recent progress in the growth and processing of nitride materials In particular we have been successful in developing growth of high quality quantum well structures and novel contact layers, the creation of new wet and dry etching chemistries ,achievement of implant doping and isolation of GaN and use of these advances in fabrication of some potentially useful new device structures.

III-V NITRIDE EPITAXY

Our efforts have focused on growth of the nitrides by Metal Organic Molecular Beam Epitaxy(MOMBE) on a variety of substrates, including Al_2O_3, ZnO, GaAs, GaP and Si[7-10]. Triethylgallium (TEG), trimethylamine alane (TMAAl) and trimethylindium (TMI) are used as the Ga, Al and In sources, respectively, and are transported with either H_2 or He carrier gas. Nitrogen was derived from a nitrogen plasma generated from N_2 at 200W in a Wavemat ECR source . Growth rates are typically in the range 0.3-0.7 μm/hr . The GaN is grown at 700°C producing the cubic phase on GaAs substrates ,whereas higher temperature growth leads to hexagonal material. Our material is usually resistive as-grown. InN is typically deposited at 500°C and is strongly n-type (10^{20} cm^{-3}) due to auto-doping ,whereas AlN is grown at 700°C and is invariably semi-insulating. The ternary materials InGaN and InAlN have been produced for all x-values[11]. The autodoping in these layers decreases for lower In contents ,with the

DISCLAIMER

Portions of this document may be illegible in electronic image products. Images are produced from the best available original document.

InAlN becoming resistive for x<0.35. For InGaN however the doping persists to lower In contents, ~0.5.

Though Mg has been shown to produce p-type doping in GaN, it has a relatively large ionization level. ~0.16 eV. At room temperature therefore only ~$3x10^{-3}$ of the Mg acceptors are ionized so that maximum doping levels of ~10^{18} cm^{-3} are achieved and in general p-doping is limited to the 10^{17} cm^{-3} region. This has serious consequences for achieving good ohmic contacts to p-type GaN. A search for other possible acceptor dopants is highly desirable . Because carbon is such an effective acceptor in GaAs and GaP[12] grown by MOMBE (and MOCVD) we have explored its properties in GaN. The extremely low decomposition efficiency of TMG means that halocarbon sources are needed for controlled carbon incorporation. We have grown GaN doped with C from a CCl4 source and find an almost linear increase in hole concentration as the CCl_4 flow increases[9]. Unfortunately the addition of CCl_4 to the growth chemistry reduces the GaN growth rate due to the presence of parasitic etching reactions. For example the undoped growth rate of ~0.8 μm/hr is reduced to effectively zero at a halocarbon flow of 1.1 sccm. Chlorine -containing plasma chemistries are effective in dry etching of GaN, with the etch products expected to be $GaCl_x$ and NCl_3. It remains to be seen whether other halocarbon gases such as CBr_4 will provide a wider growth window in order to allow achievement of higher of higher p-type doping levels.

As an example of the quality of state -of -the -art nitride growth , Figure 1 shows a TEM cross-section of a structure grown by MOMBE on an Al_2O_3 substrate . Due to the large lattice mismatch between the substrate and the AlN layer there is a high density ($10^{11}cm^{-3}$) of threading dislocations and other defects such as stacking faults . Note that subsequent growth of GaN produces a planarizing effect, leading to InGaN quantum wells with excellent definition and interfacial smoothness . Although many research efforts are now directed at solving the issue of lack of a suitable lattice-matched substrate for GaN, the defects in this material do not appear to degrade its optical properties and currently all commercial GaN-based LEDs are grown on Al_2O_3. [2]. The excellent long-term reliability of these devices also indicates that dark-line defects are not a factor in GaN.

PROCESSING

1. ION IMPLANTATION DOPING

The use of ion implantation for selective area doping or isolation is a critical requirement for the advancement of GaN device technology. To date there has been little work in this area and generally implantation has been used to introduce impurities for study of their optical properties. Maruska and Tiefjen have shown that GaN LEDs emit at 430 nm (violet) when implanted with Mg and at 590 nm (yellow) when co-implanted with Mg and Zn . The use of Zn doping alone produced green emission . Diffusion studies of implanted dopants have shown there is no measurable diffusion at 900C of any species expect S in GaN. [14].

Figure 2 shows the sheet resistance of material implanted with Si^+, Mg^-, $Mg^- P^+$ or unimplanted. as a function of annealing temperature . Above 1050°C, the Si^+ becomes electrically active with an efficiency of ~90% for a dose of $5x10^{14}$ cm^{-2}. Mg^+ implantation alone did not produce p-type doping, but when co-implanted with P^- we obtained a sharp n-to-p conversion of the GaN at 1050°C with an activation efficiency of ~60% at a dose of $5x10^{14}$ cm^{-2}. Annealing by itself above 1000°C produced a slight increase in n-type conductivity in GaN ,which may result from creation ,or depassivation of the defects responsible for the as-grown doping(i.e. N-vacancy -related defects or chemical impurities such as O or Si.

2. ION IMPLANTATION ISOLATION

Both n-type and p-type GaN can be efficiently isolated by the type of multiple energy implant schemes used for more conventional III-V materials . We have achieved maximum sheet resistances >$5x10^9$ ohms/square in both conductivity types, after a multiple energy N^+ implant (50-250 keV) at doses of 2-$6x10^{13}$ cm^{-2} and subsequent annealing at ~750°C[15]. Arrhenius plots of conductivity in isolated GaN can be used to determine the energy level of the main defect introduced by this implant /anneal sequence. The activation energy for the p-type material is 0.90 eV and that for the n-type GaN is 0.83 eV. These energy values represent the approximate position of the Fermi level and show why very high resistances can be obtained in implant-isolated GaN. However ,an optimum situation is to produce midgap levels in isolated material, i.e. at ~1.6 eV in GaN. The

microstructural nature of the defects responsible for the carrier compensation is not known at this point but is likely to consist of native defect complexes. In both n- and p-type GaN ,these complexes anneal out above ~750°C.

Similar experiments have been performed with n-type layers of InAlN and InGaN. Sheet resistances of $>10^8$ ohm/square were obtained for N^+ implanted InAlN, whereas in InGaN, sheet resistances typically 50-100 times higher than the as-grown values were obtained with N^+, O^- or F^+ implantation. Figure 3 shows the evolution of normalized sheet resistance in O^+ implanted $In_{0.75}Al_{0.25}N$ with subsequent annealing. The sheet resistance increases up to ~600°C and then is reduced to the original unimplanted values at ~800°C. This behavior is typical of that seen in other III-V semiconductors, and is caused by the introduction of deep acceptor states related to the implant damage that compensate the shallow native donors[16]. This produces an increase in sheet resistance of the material ,the magnitude of which is dose-dependent. The usual situation is that all of these are compensated but some residual conductivity remains due to the presence of inter-defect hopping of trapped carriers from one closely-spaced trap site to another, i.e. there is an excess of deep states over that required for optimum compensation . Subsequent annealing removes these excess states, leading to an increase in sheet resistance of the material. Continued annealing above ~600°C for $In_{0.75}Al_{0.25}N$ reduces the deep acceptor concentration below that required to trap all of the original free electrons and the conductivity increases back to the pre-implanted value . In this material ,annealing above 800°C actually produces a sheet resistance lower than in the as-grown samples, due either to loss of nitrogen from the uncapped material or the existence of additional donor states created by the implantation . In InAlN ,optimum implant/anneal schemes produce material with activation energies <0.6 e v, i.e. again they are not at midgap . Even lower activation energies (<0.4 eV) are obtained in InGaN ,and combined with its smaller bandgap ,means that isolation is less effective in these alloys.

3. DRY ETCHING

Due to the inert chemical nature of the nitrides, patterning by wet chemical etching has proven difficult. Relatively low etch rates have been reported for GaN(<500Å/min) under reactive ion etching conditions[17,18],however significantly higher etch rates (1000-4000 Å/min) have been obtained in high density plasmas under moderate dc-bias conditions[19,20]. For example, Electron Cyclotron Resonance(ECR) sources provide a high ion density with controllable dc-biasing to minimize plasma-induced damage. Other high density configurations include Inductively Coupled Plasmas(ICP), Helicon, Helical Resonator and magnetron-enhancement. The plasma chemistries attempted for the nitrides include Cl_2/H_2, BCl_3, CCL_2F_2, CH_4/H_2, $SiCl_4$, HBr, HI and $Cl_2/CH_4/H_2/Ar$. The group III elements can be removed as volatile chlorides .bromides or iodides or as metalorganics while the nitrogen can be removed as NH_3, NF_3 or NCl_3. The bond strengths of the nitrides are quite high relative to other III-V compounds, and therefore a significant physical component is required in addition to the chemistry discussed above.

Figure 4(top) shows etch rates of GaN and AlN as a function of sample temperature in ECR $Cl_2/CH_4/H_2$ Ar or $Cl_2/H_2/Ar$ plasmas(850W of microwave power, 1 mTorr process pressure and 180 V dc bias). There is little temperature dependence for these materials, although for InN the etch rates increase rapidly above ~150°C. The bottom of Figure 4 shows Auger Electron Spectroscopy surface scans of GaN before exposure to the plasma ,and after etching at either 30° or 170°C. Within experimental error there is no change in the stoichiometry of the GaN surface . However at very high microwave power levels or rf biases there can be preferential loss of N, leaving a Ga-rich surface.

In the etch chemistries employed to date selectivities for removing one nitride relative to another have not been particularly high(typically less than a factor of 3), so more work is needed on developing higher selectivity. Secondly, there has been little effort on measuring plasma-induced damage in the nitrides . From ion implantation studies it is clear that these materials are very resistant to damage, but some quantification of this phenomenon during ECR or RIE is needed Thirdly, it is also of interest to directly identify the etch products from the nitrides ,and in particular to see the relative importance of the various N species when both Cl_2 and H_2 or Cl_2 and F_2 are present in the plasma chemistry.

We note finally that ion milling rates for the nitrides are a factor 2-3 slower than for materials like GaAs and InP ,indicating that there must be a chemical component present in order to achieve

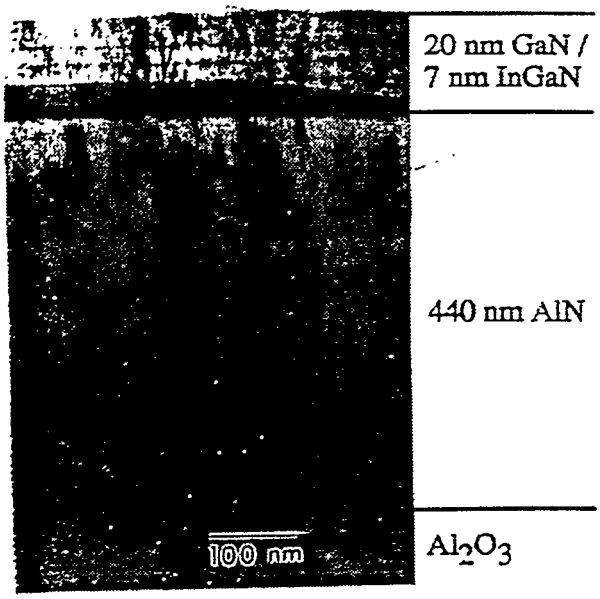

Figure 1. TEM cross-sections of a multiple InGaN/GaN quantum well structure on an AlN buffer.

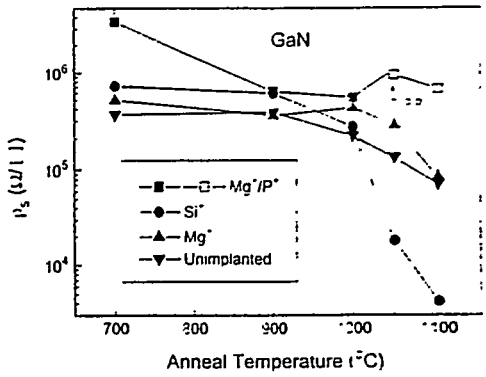

Figure 2. Sheet resistance as a function of annealing temperature for unimplanted GaN and material implanted with Si−, Mg+ or Mg+/P−.

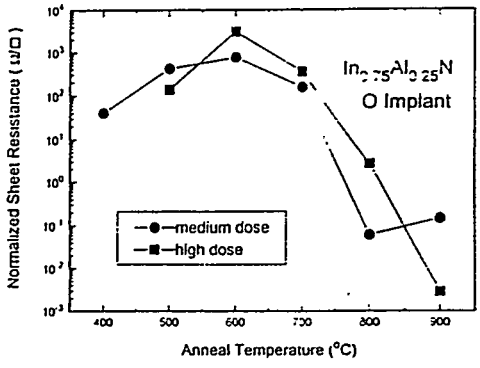

Figure 3. Sheet resistance as a function of annealing temperature for O+ implanted $In_{0.75}Ga_{0.25}N$.

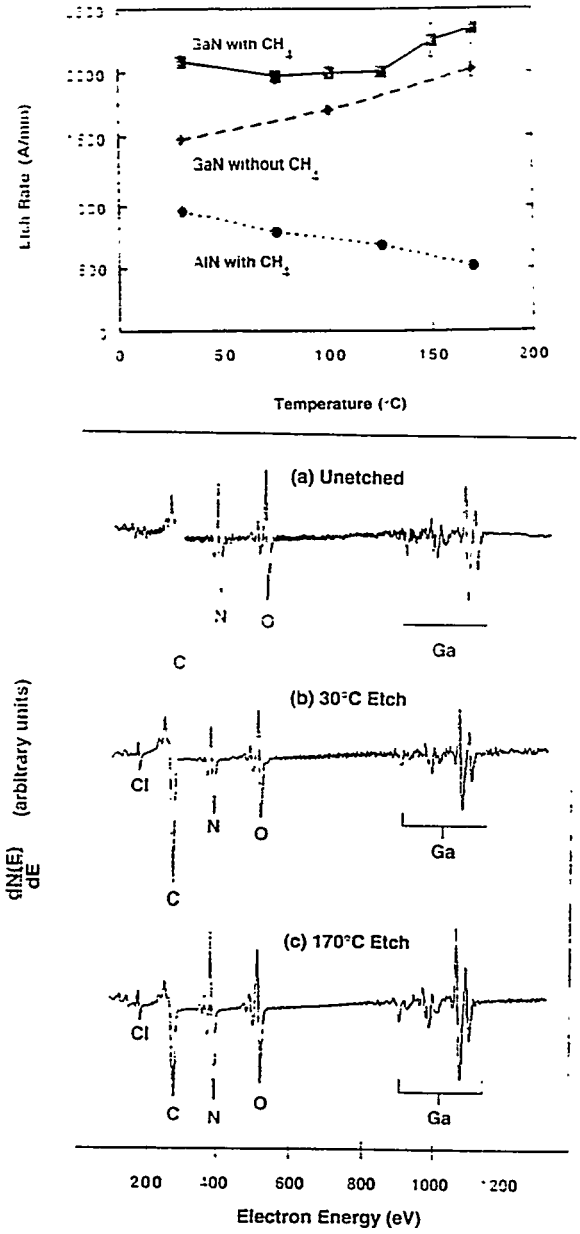

Figure 4. Etch rates of GaN and AlN versus temperature in ECR Cl2/CH4/H2/Ar discharges (top) and AES spectra of GaN(bottom) before and after etching at different temperatures.

practical etch rates . In ion milling the removal rate of most mask materials is faster than the etch rates of the nitrides, limiting this technique to formation of shallow features.

4. WET CHEMICAL ETCHING

There were several early reports of wet etching of GaN in NaOH. which progressed by formation of an insoluble gallium hydroxide (GaOH) coating [21,22]. This film had to be removed by continual jet action. Others have reported that H_3PO_4 will remove GaN.[23] A variety of different etch solutions have been employed for amorphous or polycrystalline AlN, including hot (85 C) H_3PO_4[24,25], boiling HF/H_2O[26], HNO_3/HF[27] or dilute NaOH solutions[18]. However there do not appear to be reliable for single crystal material. For InN. aqueous KOH and NaOH solutions were found to produce etch rates of a few hundred angstroms per minute at 60°C[29].

We have found that a common photoresist developer solution AZ400K produces controlled, reliable wet etching of single crystal AlN at a rate whose absolute magnitude depends strongly on the crystalline quality of the material. Figure 5 shows the etch rate versus inverse temperature for three different AlN samples, one of which is polycrystalline and the other two are single crystal of different quality. .The etching is thermally activated with the same activation energy of 15.5 kCal/mol in all cases . The rate was not sensitive to agitation and was dependent on the etchant concentration. These are characteristics of reaction-limited etching of the form

$$R=R_0 \exp(-E_a/kT)$$

We find that R_0, an attempt frequency for reaction between the (OH-) ions and the AlN surface, is strongly dependent on material quality. A great deal more work needs to be done to develop reliable wet etches for GaN, InN and the ternary alloys in order to accelerate nitride device technology.

MICRODISK LASERS

The ultimate aim of much of the nitride work at present is a junction diode laser, but there are alternative optically active microstructures which may have application in future photonic or optoelectronic circuits. One of these is the whispering -gallery -mode microdisk laser, which makes use of optical modes at the edge of a thin semiconductor dielectric disk 2-10 μm in diameter which is suspended in air or a low refractive index medium such as SiO_2[30]. Optical gain is provided by one or more optically or electrically pumped InGaN quantum wells in the plane of the disk. The optical mode is strongly confined in the direction perpendicular to the thin disk.

Figure 6 shows a schematic of the process sequence for a microdisk GaN-based laser. First a quantum well structure consisting of InGaN quantum wells with GaN cladding layers is patterned with circular masks, and then dry etched down to the substrate. The AlN buffer layer is then selectively undercut to form the pedestal structure . SEM micrographs of such a structure at various stages of fabrication are shown in Figure 7. The GaN/InGaN QW are grown by MOMBE on an AlN buffer. Dry etching is performed with an ECR $CH_4/Cl_2/H_2/Ar$ plasma at 850 W microwave power, 1 mTorr pressure and 150 W of rf-power. The SEM picture at the top of Figure 7 shows the etching has intruded ~500Å into the Al_2O_3 substrate. The disk is formed by selective etching of the AlN in AZ400K solution.

Similar structures can be fabricated in which the InGaN/GaN quantum wells are replaced by Er-doped GaN layers. The Er can be incorporated during growth or by direct implantation . Figure 8 shows a SIMS profile of Er after implantation into GaN and subsequent annealing at 650°C. It is usually necessary to co-implant oxygen to achieve good emission at 1.54 μm from the Er^{3+} states. The implanted Er does not diffuse during the annealing step[31]. The resulting structure can then be fabricated into a microdisk using a similar procedure to that described previously. A schematic of this process is shown in Figure 9. The effect of the microdisk geometry is to enhance the luminescence at 1.54 μm and the advantage of the wide bandgap host for the Er is that the luminescence is less sensitive to temperature and does not fall-off as quickly with increasing temperature as does the output from a conventional junction diode laser. Such structures may therefore be useful in applications requiring elevated temperature operation.

InN CONTACT HBTs

Carbon-doped base heterojunction bipolar transistors (HBTs) in the GaAs/AlGaAs system display much better stabilities under bias-stress aging

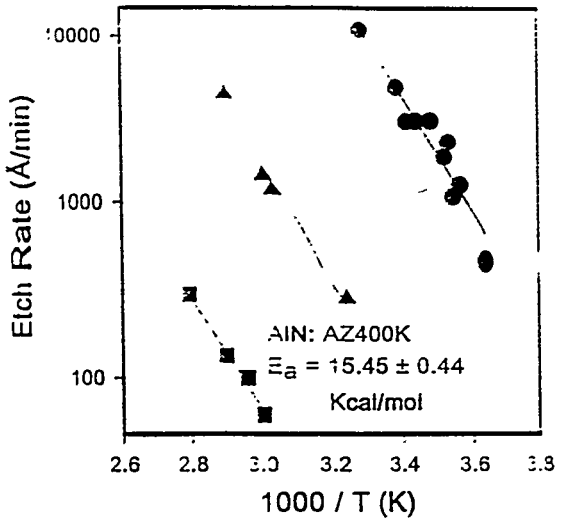

Figure 5. Arrhenius plot of etch rate of AlN samples in AZ400K solution . The best quality single crystal has the slowest etch rate .while the polycrystailine material has the fastest rate.

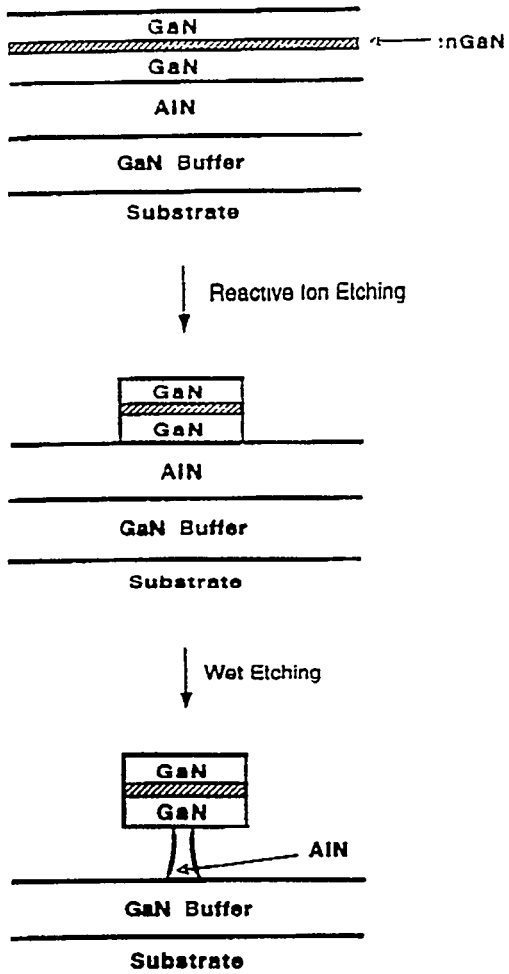

Figure 6. Schematic of process sequence for a InGaN/GaN microdisk laser

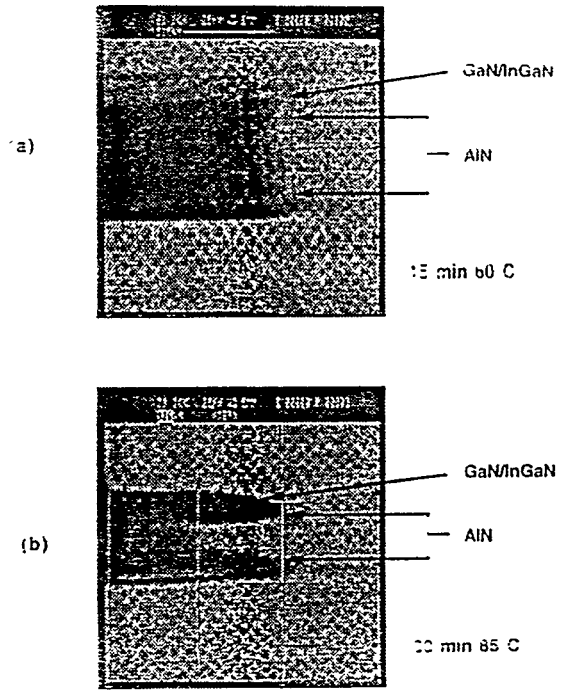

Figure 7. SEM micrographs of a microdisk laser structure at various stages of the process.

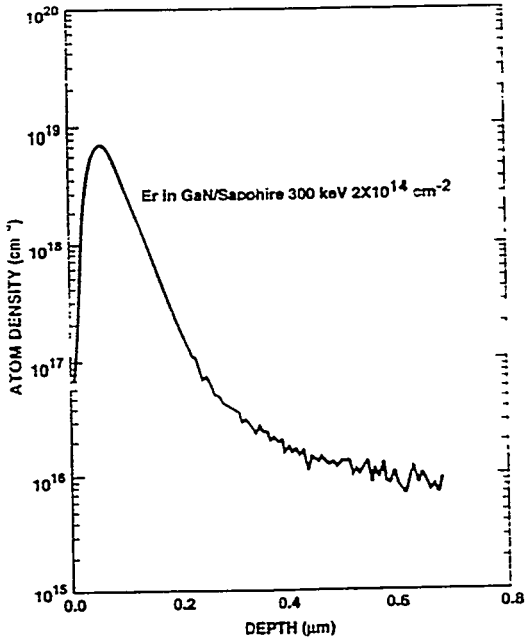

Figure 8. SIMS profile of implanted Er in GaN after annealing at 650 C

than devices using Be, Mg or Zn for p-type doping[32]. One of the most important parameters for achieving high speed performance in digital applications is the emitter resistance ,and the InGaP or AlGaAs emitter layer is generally capped with highly doped GaAs/InGaAs graded out to InAs to provide a low bandgap layer for subsequent metallization. The InAs can be doped with Sn to achieve high ($n=3x10^{19}$ cm^{-3})conductivity, with typical contact resistivities of $5x10^{-7}$ ohm-cm^2 for TiPtAu nonalloyed metallization[33]. However, the InAs critical layer thickness is generally exceeded in practical HBT structures, leading to rough surface morphologies. This is a potential problem for small emitter dimensions devices since some contacts would potentially be placed in regions of thinner InAs and therefore, poorer contact resistance.

Recently, low contact resistivities have been reported for nonalloyed TiPtAu metallization on unintentional doped InN grown by MOMBE[34]. The polycrystalline InN is grown at 500°C ,consistent with the growth temperature of high performance GaAs/AlGaAs or GaAs/InGaP HBTs for both digital and power applications ,and the surface morphology of the InN is much smoother than that of InAs-based emitter contact structures. We have demonstrated nonalloyed TiPtAu contacts with excellent contact resistivities($5x10^{-7}$ ohm-cm^2).

The HBT structures were grown by MOMBE on semi-insulating GaAs substrates. The structure was completed in one of two different ways. In the first, 1200Å of InN($n=5x10^{20}$ cm^{-3}) was grown, while in the second the GaAs was graded through InGaAs to InAs (300 Å, $N=1.5x10^{19}$ cm^{-3}) to the 1200Å InN layer. The entire structure was grown at 500°C using all-gaseous sources, as described previously[34].

Nonalloyed ohmic contacts were formed to the two types of structures using e-beam deposited Ti(500Å)/Pt(750Å)Au(3000Å) patterned by lift-off. HBTs with 2x5 μm^2 emitter dimensions were fabricated using a dry-etched self-aligned process, and this mask set also contained transmission line patterns for determination of contact resistivity.

A contact resistivity of $2\text{-}5x10^{7}$ ohm-cm^2 was obtained for both InN-based contact schemes, but superior performance was displayed by the graded structure . This was ascribed to the formation of GaN at the interface between the abrupt InN/GaAs structure which degraded the contact properties [35]. A Gummel plot from an HBT structure fabricated with the new InN/InGaAs/GaAs emitter contact is shown in Figure 10. The maximum dc gain was 35 for 2x5 μm^2 devices. No change in device characteristics was observed during aging at 25°C for 90 h at an emitter current density of $4x10^{4}$ A/cm^2. TEM pictures showed the uniform nature of the InN whereas the more conventional InGaAs/GaAs emitter contacts showed very rough surfaces for the InAs.

While TiPtAu metallization on these structures also yields nonalloyed ohmic contact resistivities of $5\text{-}7x10^{-7}$ ohm-cm^2, there is one significant concern about contact uniformity for submicron dimension devices. Therefore ,the InN-based contact structure is likely to be a superior alternative for small mesa HBTs. The drawback of the InN -based contacts is that they suffer from deterioration in both morphology and contact resistance above 400°C, whereas the InAs -based layers are stable to 500°C. One must therefore reduce the thermal budget during of the former and in particular adjust the implant isolation conditions so that lower annealing temperatures than currently used can be employed.

LATTICE MATCHED NITRIDES ON Si

A severe shortcoming for rapid exploitation of nitrides in high power electronics is lack of a homoepitaxial substrate . Growth on Si offers many advantages, as listed in Table 1. Lattice matching is possible for mixed group V nitrides, as shown in Table II. Part of the difficulty in achieving lattice matching is the need for accurately controlling and changing the As or P fluxes in conventional MBE ,where the effusion ovens have long thermal time constants. This can be overcome with use of gaseous group V sources such as AsH_3 and PH_3, as in MOMBE. In MOCVD, the growth of mixed group V materials is complicated by two major problems. The need to use high growth temperatures to decompose the NH_3 makes growth of In-containing compounds difficult due to desorption of In from the surface above ~540°C. As seen from Table II, high In concentrations are required to achieve lattice matching to Si. A second problem is that MOCVD suffers from pre-reactions in the gas phase which makes compositional control of mixed group V alloys difficult. Because MOMBE is not limited to high temperature sources and does not suffer from gas-phase interactions, neither of these problems occurs to any great extent.

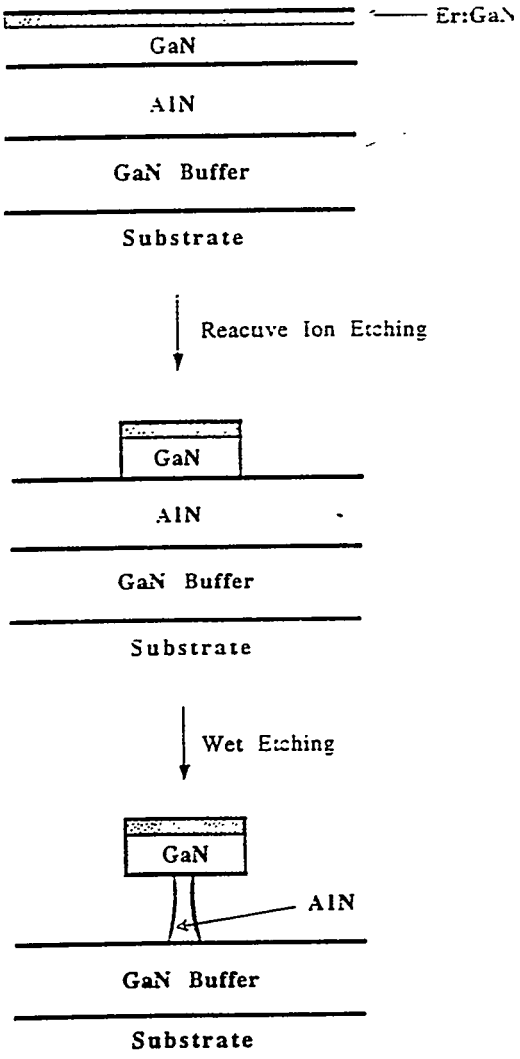

Figure 9. Schematic of process sequence for Er-doped microdisk structure.

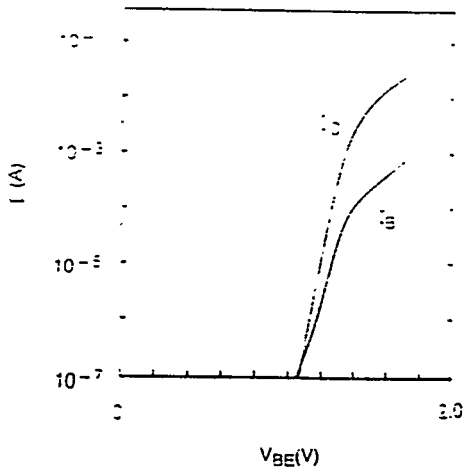

Figure 10. Gummel plot of a 2x5 μm^2 emitter dimension HBT with InN contacts.

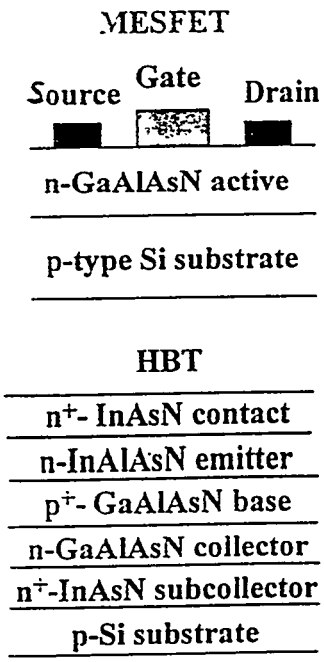

Figure 11. Potential layer structures for MESFET or HBT based on mixed group V nitrides lattice matched to Si

DISCLAIMER

TABLE I: Advantages of Mixed Group V Materials on Si:

1. Cheap substrates
   2 inch diameter:
   $7-20 for Si vs. $135-400 for sapphire or ~$800/sq. in. for SiC
2. Large area deposition:
   6-12 inch substrates commercially available
3. Cubic substrate
   Easier to cleave laser facets or to dice circuit chips
4. Lattice matched layers possible (see Table I)
   Improved material quality relative to highly mis-matched systems
5. Wide range of bandgaps available (see Table II)
   Potential for fabrication of full range (red - blue) of optical devices
6. Integration with Si electronics
   Potential for fabrication of optoelectronic circuits on Si
   Potential for fabrication of mixed digital/power circuits on Si

Table I. Approximate compositions and bandgaps of materials lattice matched to Si assuming Vegard's law. For comparison, the bandgaps of GaAs and AlAs are 1.42 eV (direct) and 2.14eV (indirect) respectively. Values for the band structure of AlN were taken from recent theoretical calculations of Dr. Arden Sher and colleagues at SRI Int.

Lattice Matched Material	Expected Type of Bandgap	Bandgap (eV)
$GaAs_{0.8}N_{0.2}$	Direct	1.8
$AlAs_{0.83}N_{0.17}$	Indirect	2.8
$Ga_{0.7}Al_{0.3}As_{0.81}N_{0.19}$	Direct	2.4
$InP_{0.51}N_{0.49}$	Direct	1.77
$InAs_{0.42}N_{0.58}$	Direct	1.43

Another major obstacle to developing a Si-based technology is lack of information about the variation of critical material properties such as bandgap and quaternary alloy composition. Due to alloy bowing ,it is not known exactly which compositions will provide the combination of electronic structure ,lattice constant and thermal behavior needed for fabrication of high performance devices. In addition there are indications of a miscibility gap for GaAsN, in which only limited quantities of N can be incorporated into GaAs and As into GaN. One group has reported substantial concentrations of N in GaAs, but indicated formation of two distinct phases under these conditions[36]. More effort is needed to establish the solubility limits for N in the group V nitrides. Figure 11 shows typical MESFET and HBT structures based on mixed group V nitrides lattice matched to Si substrates. If growth of the appropriate compositions is possible, these devices are expected to have a significant impact in power applications.

CONCLUSIONS

The large bandgaps, thermal and chemical stability ,excellent transport properties and good thermal conductivities of the III-V nitrides offer many opportunities for fabrication of novel photonic and electronic devices. Considerable progress has been made in recent times on the growth of these materials and in developing the process modules. Much more effort is required on ohmic contacts, substrate development ,implantation, p-type doping during epitaxial growth and growth of ternary compounds.

ACKNOWLEDGMENTS

The work at UF is supported by a grant from the Division of Materials Research (LaVerne Hess), an AASERT grant through ARO, a University Research Initiative administered through ONR (A. Goodman). The work at Sandia is supported by DOE contract no. DE ACO4-94AL85000. The work at Hughes is partially supported by an ARO contract. The technical assistance of the staff of the MicroFabritech facility (UF), P. L. Glarborg and J. Escobedo (Sandia) and J. D. MacKenzie, C. B. Vartuli and J. R. Mileham(UF) is greatly appreciated.

REFERENCES

[1].H.Morkoc,S.Strite,G.B.Bao, M.E.Lin, B.Sverdlov and M.Burns, J.Appl.Phys. 76 1363 (1994)

[2]. S.Nakamura, T.Mukai and M.Senoh, Appl. Phys. Lett. 64 1687 (1994)

[3].B.Goldenberg, J.D.Zook and R.J.Ulmer ,Appl.Phys.Lett.62 381 (1993)

[4].S.C.Binari,L.B.Rowland.W.Kruppa.G.Kelner.K. Doverspike and D.K.Gaskill.Electronics Lett. 30 1248(1994)

[5].M.A.Khan,A.Battarai,J.N.Kuznia and D.T.Olson.Appl.Phys.Lett. 63 1214 (1993)

[6]M.A.Khan,M.S.Shur,J.N.Kuznia,Q.Chen,J.Burm and W.Schaff,Appl.Phys.Lett.66 1083 (1995)

[7]C.R.Abernathy.F.Ren and S.J.Pearton,J.Vac.Sci.Technol.B11 179(1993)

[8]C.R.Abernathy.J.D.MacKenzie,S.Bharatan,K.S.Jo nes and S.J.Pearton.Appl.Phys.Lett.66 1632(1995)

[9]C.R.Abernathy.J.D.MacKenzie ,S.J.Pearton and W.S.Hobson,Appl.Phys.Lett.66 1969 (1995)

[10]C.R.Abernathy .Proc.21st SOTAPOCS Conf.(Electrochemical Society Meeting,Miami.FL Oct.1994),Proc.Vol.94-34 12 1995)

[11]C.R.Abernathy.S.J.Pearton,J.D.MacKenzie,S.Bh aratan and K.S.Jones,41st Nat.Symp.Am.Vac.Soc.Denver ,CO,Oct.1994;J.Vac.Sci.Technol.A(in press).

[12]C.R.Abernathy.Inst.Phys.Conf.Ser.129 663 (1993)

[13]H.P.Maruska and J.J.Tiefjen,Appl.Phys.Lett.15 327(1969)

[14]R.G.Wilson,S.J.Pearton,C.R.Abernathy and J.M.Zavada,Appl.Phys.Lett. 66 2238(1995)

[15]J.C.Zolper,S.J.Pearton,C.R.Abernathy and C.B.Vartuli,Appl.Phys.Lett.66 3010(1995)

[16]S.J.Pearton,Mat.Sci.Rep.4 313 (1990)

[17]I.Adesida,A.Mahajan,E.Andideh,M.A.Khan,D.T. Olsen and J.N.Kuznia,Appl.Phys.Lett.63 2777(1993)

[18]M.E.Lin,Z.F.Fan,L.H.Allen and H.Morkoc,Appl.Phys.Lett.64 887 (1994)

[19]S.J.Pearton,C.R.Abernathy and F.Ren,Appl.Phys.Lett,64 2294 (1994)

[20]R.J.Shul,S.P,Kilcoyne,M.H.Crawford,J.E.Parmet er,C.B.Vartuli,C.R.Abernathy and S.J.Pearton,Appl.Phys.Lett.66 1761 (1995)

[21]T.L.Chu,J.Electrochem.Soc.118 1200(1971)

[22]J.I.Pankove,J.Electrochem.Soc.119 1118(1972)

[23]A.Shintani and S.Minagawa,J.Electrochem.Soc.123 706(1976)

[24]T.Y.Sheng,Z.Q.Yu and G.J.Collins,Appl.Phys.Lett.52 576(1988)

[25]T.Pauleau,J.Electrochem.Soc.129 1045 (1982)

[26]G.Long and L.M.Foster,J.Am.Ceram.Soc.42 53 (1959)

[27]C.R.Aita and C.J.Gawlak,J.Vac.Sci. Tech.A1 403(1983)

[28]G.R.Kline and K.M.Lakin,Appl.Phys.Lett.43 750(1983)

[29]Q.X.Guo,O.Kato and A.Yoshida,J.Electrochem.Soc.139 2008(1992)

[30]S.L.McCall,A.F.J.Levi,R.E.Slusher,S.J.Pearton and R.A.Logan,Appl.Phys.Lett.60 289(1992)

[31]R.G.Wilson,R.Schwartz,C.R.Abernathy,S.J.Peart on,N.Newman,M.Rubin,T.Fu and J.M.Zavada,Appl.Phys.Lett.65 992(1994)

[32]F.Ren,T.Fullowan,J.Lothian,P.Wisk,C.R.Abernat hy,R.Kopf,S.Downey and S.J.Pearton,Appl.Phys.Lett.59 3613 (1991)

[33]F.Ren,C.R.Abernathy,S.J.Pearton.T.Fullowan.J.L othian,P.Wisk,Y.K.Chen,W.S.Hobson and P.Smith,Electronics Lett.27 2391(1991)

[34]C.R.Abernathy,Mater.Res.Soc.Symp.Proc.240 3 (1993)

[35]F.Ren,C.R.Abernathy,S.N.G.Chu,J.R.Lothian and S.J.Pearton,Appl.Phys.Lett.66 1503 (1995)

[36]J.W.Orton,D.Lacklison.N.Baba-Ali,C.T.Foxon,,T.Cheng,S.Novikov,D.Johnston.S.Ho oper,L.Jenkins,L.Challis and T.L.Tansley,J.Electron.Mater.24 263(1995)